



ORIGINAL ARTICLE

Efficient reduction of NO_x emissions from waste double-base propellant in co-pyrolysis with pine sawdust



Guorui Jin, Moru Wang, Jianwei Zhang, Ling Chen, Xin Liao, Weidong He*

School of Chemistry and Chemical Engineering, Nanjing University of Science and Technology, Nanjing 210094, China
Key Laboratory of Special Energy Materials, Ministry of Education, Nanjing 210094, China

Received 28 November 2022; accepted 29 January 2023
Available online 3 February 2023

KEYWORDS

Waste double-base propellant;
Pine sawdust;
Co-pyrolysis;
Reaction kinetics;
NO_x emission

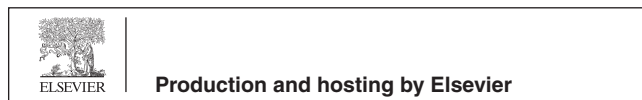
Abstract Co-pyrolysis technology containing biomass offers remarkable advantages in reducing NO_x emissions economically and efficiently. In this work, it was innovatively introduced to solve the problem of excessive NO_x emission during the incineration of waste energetic materials (EMs). The kinetics and NO_x emission characteristics of waste double-base propellant (DP), pine sawdust (PS), and their mixtures with different ratios during pyrolysis were investigated by thermogravimetric analysis and fixed-bed experiments. The results showed that there was a significant interaction between DP and PS. Kinetic analysis by Friedman and Kissinger-Akahira-Sunose (KAS) methods demonstrated that the average activation energies of the mixtures with different ratios were smaller than that of DP, indicating that the addition of PS improved the reactivity of co-pyrolysis. In addition, the fixed-bed experiment determined that the lowest NO_x emission was achieved during DP pyrolysis alone at 900 °C. Co-pyrolysis at this temperature was found to have synergistic effects of reduced NO_x emissions for different ratios of mixtures. The best synergistic effect was achieved at the mixing ratio of 60 wt% DP and 40 wt% PS, resulting in a 72.11 % reduction in actual NO_x emissions compared to the expected value. This study provides a new direction and powerful data support for the clean, efficient and economic treatment of waste EMs, especially for practical engineering strategies.

© 2023 The Author(s). Published by Elsevier B.V. on behalf of King Saud University. This is an open access article under the CC BY-NC-ND license (<http://creativecommons.org/licenses/by-nc-nd/4.0/>).

* Corresponding author at: School of Chemistry and Chemical Engineering, Nanjing University of Science and Technology, Nanjing 210094, China.

E-mail address: hewedong@njjust.edu.cn (W. He).

Peer review under responsibility of King Saud University.



1. Introduction

Energetic materials (EMs) are mainly used in the domain of national defense to accomplish military operations such as propulsion, projectile, and explosion (Chen et al., 2022b; Wang et al., 2022a; Wang et al., 2022b). Their storage and service life are limited. After reaching their lifespan, the EMs will become waste EMs due to the deterioration of stability and safety (Cho et al., 2020; Park et al., 2016). In general, about thousands to tens of thousands of tons of waste EMs accumu-

late annually in large military countries (Duijm, 2002). Waste EMs are worldwide hazards caused by their inflammability, explosiveness, and high NO_x emissions (Duijm and Markert, 2002). If such hazards are not handled properly, the consequences will be very serious.

Co-pyrolysis/co-combustion technologies are one of the most potential waste treatment methods, which have a broad prospect in reducing pollutant emissions (Chen et al., 2018; Liu et al., 2022; Ulusoy et al., 2021). NO_x is the key indicator of pollutant emissions (Van Caneghem et al., 2016). NO_x emissions pose a great threat to human health and the ecological environment, which must be strictly controlled and significantly reduced (Gholami et al., 2020). Currently, studies on co-pyrolysis/co-combustion technologies are mainly focused on conventional solid fuels, including coal (Bhattacharyya et al., 2021; Laougé and Merdun, 2021; Merdun and Laougé, 2021), sewage sludge (Chen et al., 2018; Ma et al., 2022; Wang et al., 2020), biomass (Liao et al., 2021; Wang et al., 2016; Yang et al., 2021a), and municipal solid waste (Peng et al., 2016; Suksankraisorn et al., 2010). Merdun et al. (Merdun and Laougé, 2021) analyzed the pyrolysis kinetics of the mixture of greenhouse vegetable waste and coal by thermogravimetry (TG). It was indicated that the mixture of the two has a synergistic effect, with the lowest activation energy at 50 wt% of each. NO_x emission characteristics during co-pyrolysis of sewage sludge with corn straw in a tube furnace showed the lowest NO_x emissions at a sewage sludge ratio of 75 wt% (Chen et al., 2018). Wang et al. (Wang et al., 2020) studied the combustion and NO_x emission characteristics of sludge, biomass, and their mixtures using TG and tube furnaces. The results showed that the combustion characteristics at 80 wt% biomass + 20 wt% sludge improved compared to the theoretical values, while NO_x emissions were the lowest. In conventional solid fuels, the fuel nitrogen content varies little, usually not exceeding 2.5 wt%. And the fuel nitrogen is first produced as HCN and NH_3 (Glarborg et al., 2003). In contrast, the nitrogen content of most EMs is more than 12 wt%, and nitrogen mainly exists in the form of O- NO_2 or N- NO_2 (Yan et al., 2009a; Yan et al., 2009b). In this way, NO_2 is first generated during the combustion of EMs, leading to serious exceedances of NO_x emissions (Baxter et al., 1996; Buckley et al., 1997). There are significant differences in composition and structure between EMs and conventional solid fuels, which will have a great impact on the whole pyrolysis/combustion process after mixing. Therefore, co-pyrolysis/co-combustion technologies of EMs with conventional solid fuels will be a valuable research direction.

NO_x emissions tend to decrease with NH_i radical concentration (Abelha et al., 2008), and char reduction reactivity to NO (Yang et al., 2021b), which is revealed in co-pyrolysis and co-combustion studies. Biomass has the characteristics of high H/C, O/C, volatile content, low ignition temperature, and generally low sulfur and nitrogen content, which has attracted more and more attention in the field of waste cleaning treatment (Laougé and Merdun, 2021). However, research in the field of EMs mainly focuses on co-combustion with coal, and there are no reports on co-pyrolysis with biomass. Wei et al. (Wei et al., 2019) found that the composite propellant, as one type of EMs, with a very low price could promote the oxidation and ignition of anthracite through the combination of thermogravimetry and Fourier transform infrared spectrometer (TG-FTIR). Ananiev et al. (Ananiev et al., 1997) investigated the co-combustion of composite propellant and coal peat by the fixed bed reactor. The results showed that NO_x emissions can be reduced almost to the level of conventional solid fuels during co-combustion. It is generally accepted that biomass produces a greater NH_3/HCN ratio than coal (Abelha et al., 2008; Tchaptada and Pisupati, 2014). NH_3 plays a crucial role in the denitration process as a reducing agent (Van Caneghem et al., 2016). Therefore, it is necessary to comprehensively study the kinetics and NO_x emission characteristics of EMs and biomass during co-pyrolysis. In addition, compared with urea and other chemicals used to reduce NO_x emissions, as well as catalysts used to promote NO_x reduction in the current incineration of waste EMs, biomass is one of the most abundant renewable energy sources in the world, with a

very low price (Laougé and Merdun, 2021). Hence, co-pyrolysis technologies of EMs and biomass can also reduce the cost of waste clean treatment to a great extent.

Double-base propellants occupy an important position in EMs (Li et al., 2021; Yan et al., 2009a; Yan et al., 2009b). In this paper, waste double-base propellant (DP) and biomass pine sawdust (PS) were selected for co-pyrolysis studies. The pyrolysis behaviors of DP, PS, and their mixtures with different ratios were studied by thermogravimetric analysis (TGA) and the pyrolysis kinetics were calculated using the Friedman and Kissinger-Akahira-Sunose (KAS) methods. Furthermore, the NO_x emission characteristics were evaluated by fixed-bed experiments. The temperature conditions for the lowest NO_x emissions during DP alone pyrolysis were found. The synergistic effect was highlighted by the deviation between the experimental and expected values of NO_x emissions during co-pyrolysis. With a view to providing a theoretical basis for the industrial application of DP-PS co-pyrolysis and control of NO_x .

2. Methodology

2.1. Materials

Waste double-base propellant (DP), mainly composed of nitrocellulose and nitroglycerin, were provided by Luzhou North Chemical Industry Co., Ltd. (Sichuan, China). Pine sawdust (PS) from Lianyungang, China. First, DP and PS were mechanically crushed. For the sake of safety, DP added an appropriate amount of distilled water during the crushing process. Then, they were dried in an oven (55 °C) for three days. Finally, the desired size range of 75–150 μm was sieved. In our work, DP and PS were mechanically mixed in certain mass ratios. The mass ratios of DP in the experimental samples were selected as 0 wt%, 20 wt%, 40 wt%, 60 wt%, 80 wt%, 90 wt%, and 100 wt%, which were denoted by PS, D2P8, D4P6, D6P4, D8P2, D9P1, and DP, respectively. To prevent moisture absorption, the prepared samples were stored in a desiccator for backup.

Due to the characteristics of inflammability and extremely fast gas production rate, the proximate analysis of DP was determined by the thermogravimetric method (Czajka, 2018). The proximate analysis of PS was performed according to ASTM standards. Their ultimate analysis and lower heating values were tested using an elemental analyzer (Thermo FLASH2000, USA) and an oxygen bomb calorimeter (SDC712, China), respectively. Test results were listed in Table 1.

2.2. Thermogravimetric analysis

Thermogravimetric analysis (TGA) experiments (PerkinElmer STA 8000, USA) were performed under an inert atmosphere (N_2). The sample mass for each experiment was 1 ± 0.05 mg. To calculate the kinetic parameters, four different heating rates (β) at 2, 5, 10, and 20 °C·min⁻¹ were selected, and the nitrogen flow rate was 20 mL·min⁻¹. A blank test was performed prior to each experiment to obtain a baseline to eliminate systematic errors in the instrument.

In order to study the interaction between DP and PS mixing, the deviation between the TG experimental value and the calculated value (ΔTG) was introduced to quantify the synergistic or inhibitory effect between the mixtures (Liao et al., 2021). A negative value of ΔTG indicates a synergistic effect,

Table 1 Proximate and ultimate analyses of the DP and PS.

Materials	Proximate analysis (wt%)				Ultimate analysis (wt%)					LHV (MJ/kg)
	M _{ad}	A _{ad}	V _{ad}	FC _{ad}	C _{ad}	H _{ad}	N _{ad}	S _{ad}	O _{ad}	
DP	0.53	0.86	98.54	0.07	22.11	2.51	14.91	0.00	60.47	8.14
PS	1.95	0.34	88.81	8.90	47.17	6.48	0.12	0.03	46.20	17.37

Mad, Aad, Vad and FCad represent the content of moisture, ash, volatile and fixed carbon on air dried basis, respectively.

Cad, Had, Nad, Sad and Oad represent the content of carbon, hydrogen, nitrogen, sulfur and oxygen on air dried basis, respectively. LHV represents a lower heating value.

while a positive value of ΔTG indicates an inhibitory effect. The calculation equation is as follows.

$$TG_{\text{cal}} = \omega_{\text{DP}} TG_{\text{DP,exp}} + \omega_{\text{PS}} TG_{\text{PS,exp}} \quad (1)$$

$$\Delta TG = TG_{\text{exp}} - TG_{\text{cal}} \quad (2)$$

where, ω_{DP} and ω_{PS} are the mass ratios of DP and PS in the mixture. $TG_{\text{DP,exp}}$ and $TG_{\text{PS,exp}}$ are the experimental TG values of DP and PS pyrolysis alone, respectively. TG_{cal} and TG_{exp} are calculated and experimental TG values of the mixture, respectively.

2.3. Kinetic analysis

The kinetic analysis is based on the Arrhenius equation (Deng et al., 2022; Laougé and Merdun, 2021), described as Eq. (3):

$$\frac{d\alpha}{dt} = A \exp\left(\frac{-Ea}{RT}\right) f(\alpha) \quad (3)$$

where α is the mass conversion ratio (%), t is the time (min), A is the pre-exponential factor, Ea is the activation energy (kJ·mol⁻¹), R is the ideal gas constant, T is the temperature (°C), and $f(\alpha)$ is the mechanical function of the reaction.

When the heating rate ($\beta = dT/dt$, °C·min⁻¹) is constant, Eq. (3) can be transformed as follows.

$$\frac{d\alpha}{f(\alpha)} = \left(\frac{A}{\beta}\right) \exp\left(\frac{-Ea}{RT}\right) dT \quad (4)$$

Eq. (5) is the integral form of Eq. (4).

$$g(\alpha) = \int_0^\alpha \frac{d\alpha}{f(\alpha)} = \frac{A}{\beta} \int_{T_0}^T \exp\left(\frac{-Ea}{RT}\right) dT \quad (5)$$

Therefore, Eq. (5) is the expression of the kinetic mechanism.

The essence of the isoconversional method is to establish the relationship between activation energy and mass conversion ratio ($Ea-\alpha$). Kinetic equations at a series of specific α describe the entire reaction process, which avoids the disadvantage of simple linear fitting with only one Ea . Since the model-free method does not consider any reaction model, errors related to the choice of kinetic model can be eliminated. For kinetic analysis, the isoconversional method used in this work was based on the model-free method Friedman (Budrugaec, 2018; Sánchez-Jiménez et al., 2013) and Kissinger-Akahira-Sunose (KAS) (Bhattacharyya et al., 2021; Laougé and Merdun, 2021), which has high reliability, and was calculated by NETZSCH Kinetics Neo software.

The Friedman isoconversional method is a widely used differentiation method (Budrugaec, 2018; Sánchez-Jiménez et al.,

2013). Unlike the conventional integration method, it provides an exact value of the Ea , even though the Ea is a function of the reaction fraction. If $f(\alpha)$ is assumed to be constant at any specific α , then $\ln(\beta \cdot d\alpha/dT)$ has a linear relationship with $1/T$. Hence, the Ea and the pre-exponential factor (A) can be obtained from the slope and intercept of the line $\ln(\beta \cdot d\alpha/dT) - 1/T$, respectively. The equation used to determine Ea is as follows.

$$\ln\left[\beta\left(\frac{d\alpha}{dT}\right)\right] = \ln[Af(\alpha)] - \left(\frac{Ea}{RT}\right) \quad (6)$$

The KAS isoconversional method is a popular integration method (Bhattacharyya et al., 2021; Laougé and Merdun, 2021). In the KAS model, Ea is obtained from the line of $\ln(\beta/T^2) - 1/T$. For a given value of α , the slope of the line is equal to $-Ea/R$. Ea is defined by the following equation.

$$\ln\left(\frac{\beta}{T^2}\right) = \ln\left(\frac{AR}{g(\alpha)Ea}\right) - \frac{Ea}{RT} \quad (7)$$

2.4. Fixed-bed experiment

To study the NO_x emission characteristics during co-pyrolysis, pyrolysis experiments of DP, PS, and their mixtures with different ratios were carried out in a fixed-bed experimental system. The system consists of a gas cylinder, mass flow controller, electric heating tube furnace, flue gas filter, buffer tank, and flue gas analyzer (MGA6, Germany), as shown in Fig. 1. Due to the fast reaction speed and gas production of DP, the buffer tank can be set to achieve smooth airflow. The MGA6 flue gas analyzer is based on the principle of non-dispersive infrared, and the sampling flow rate is about 1 L·min⁻¹. The detailed technical specifications are shown in Table S1. During the experiment, the feeding gas (N₂) flow rate was 1 L·min⁻¹, which was controlled by the mass flow controller. The set temperatures of the experiments, i.e., the center temperature of the tube furnace chamber, were 400 °C, 600 °C, 800 °C, 900 °C, and 1000 °C, measured by a thermocouple extended into the center of the furnace tube. The total mass of the samples in each experiment was 50 mg, which was repeated three times to ensure the accuracy of the experimental results.

In this experimental system, the wall and push-pull rod of the tube furnace are 310S stainless steel, and the crucible is made of corundum material, which ensures the pyrolysis safety of the propellant. A thermocouple and circulating water cooling are arranged at the inlet of the tube furnace to ensure that the inlet temperature is less than 50 °C. In this way, the crucible containing the sample before the experiment is placed at the

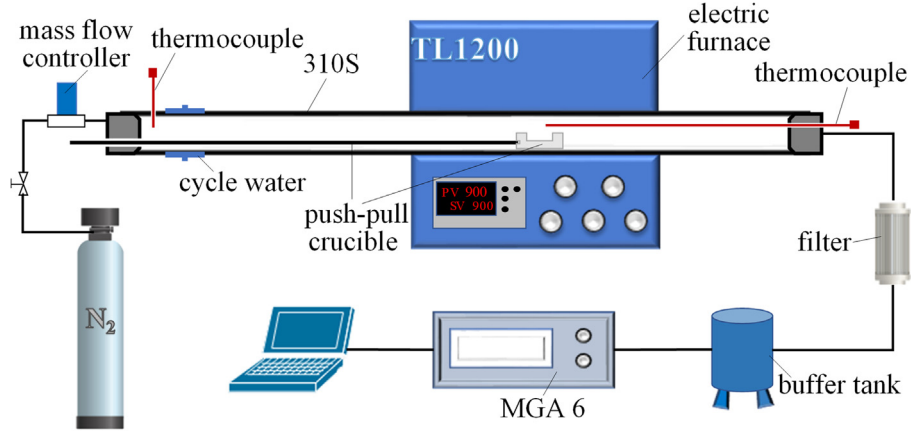


Fig. 1 Schematic diagram of the fixed-bed experimental system.

inlet of the tube furnace to prevent the decomposition of the sample before it enters the center of the chamber. The crucible is connected to the push-pull rod by means of a thread. When the gas indicator of the flue gas analyzer is stable at the set air-flow concentration, the sample is rapidly pushed into the center of the chamber through the push-pull rod. To ensure the gas tightness of the furnace chamber during the push-pull process, the push-pull rod is connected to the plug at the inlet end by a sealing ring. After one experiment, the crucible is pulled out by a push-pull rod and the ash remaining in the crucible can be further analyzed.

The actual NO_x emissions (m_{NO_x} , mg) are determined by the integral value of the gas release curve, as shown in Eq. (8).

$$m_{\text{NO}_x} = \int_{t_0}^{t_0+\Delta t} Q \cdot C_{\text{NO}_x} \cdot 46 \cdot 10^{-3} \cdot dt / (22.4 \times 60) \quad (8)$$

where, t_0 is the sampling start time (s), Δt is the sampling duration (s), Q is the sampling flow rate ($\text{L} \cdot \text{min}^{-1}$), C_{NO_x} is the instantaneous concentration of NO_x (ppm), 46 is the molecular weight of NO_x (calculated as NO_2 , $\text{g} \cdot \text{mol}^{-1}$), 22.4 is the molar volume of gas ($\text{L} \cdot \text{mol}^{-1}$).

To evaluate the interaction of DP and PS in NO_x emissions during co-pyrolysis, the expected value of NO_x emissions was introduced (Chen et al., 2018), denoted as $[m_{\text{NO}_x}]_c$. It is the weighted average of NO_x emissions, calculated by the following equation.

$$[m_{\text{NO}_x}]_c = \omega_{\text{DP}} \cdot [m_{\text{NO}_x}]_{(\text{DP})} + \omega_{\text{PS}} \cdot [m_{\text{NO}_x}]_{(\text{PS})} \quad (9)$$

where, ω_{DP} and ω_{PS} are the mass ratios of DP and PS in the mixture (wt%), $[m_{\text{NO}_x}]_{(\text{DP})}$ and $[m_{\text{NO}_x}]_{(\text{PS})}$ are the actual NO_x emissions when DP and PS are pyrolyzed separately (mg).

The deviation between the experimental and expected values of NO_x emissions was used as an evaluation criterion for the DP and PS interaction (synergy/inhibition) (Chen et al., 2018), noted as $[\text{NO}_x]_{\text{interaction}}$. It represents the percentage increase/decrease of NO_x emissions in co-pyrolysis compared to pyrolysis alone. A positive value of $[\text{NO}_x]_{\text{interaction}}$ represents that the interaction is synergistic, indicating that co-pyrolysis of DP and PS can reduce NO_x emissions. Conversely, the interaction of DP and PS co-pyrolysis on NO_x emissions is inhibitory when the $[\text{NO}_x]_{\text{interaction}}$ value is negative. The equation is as below.

$$[\text{NO}_x]_{\text{interaction}} = \frac{[m_{\text{NO}_x}]_c - [m_{\text{NO}_x}]_e}{[m_{\text{NO}_x}]_c} \times 100 \quad (10)$$

where $[m_{\text{NO}_x}]_e$ is the actual NO_x emission during pyrolysis of the mixture (mg).

2.5. Characterization of pyrolysis residue

The morphology of the residual ash was observed by a scanning electron microscope (SEM) (FEI Quanta FEG 250, USA) at an acceleration voltage of 5–10 kV after gold sputtering coating. The relative elemental content of the residue surface was determined by Energy Dispersive X-ray Spectroscopy (EDS), an accessory to SEM.

3. Results and discussion

3.1. Interaction relationship of DP and PS mixtures

The interactions of DP, PS, and their mixtures with different ratios were studied by the thermogravimetric analysis (TGA) method under an inert atmosphere (N_2) and heating rate of $20 \text{ }^\circ\text{C} \cdot \text{min}^{-1}$. Fig. 2a plotted the TG-DTG curves of DP, PS, and their mixtures with different ratios. As can be seen from the figure, there were two main stages in the weight-loss process of DP alone pyrolysis. 100–195 $^\circ\text{C}$ was the process of volatilization and thermal decomposition of nitroglycerin in DP, and 195–275 $^\circ\text{C}$ corresponded to the process of thermal decomposition of nitrocellulose in DP. The weight-loss process of PS pyrolysis alone had only one major stage, starting with thermal decomposition at 270 $^\circ\text{C}$ and ending at 430 $^\circ\text{C}$, corresponding to the release process of volatile from PS. When they were mixed in different ratios, TG and DTG curves were between DP and PS.

According to TG and DTG curves, the weight-loss process during co-pyrolysis of the mixture mainly had three stages, which correspond to the volatilization and thermal decomposition of nitroglycerin in DP, the thermal decomposition of nitrocellulose in DP, and the release of volatile in PS. The first two stages could reflect the effect of PS on DP. With the increase of PS, the peak temperature of DTG decreased gradually in the first stage and basically remained constant in the

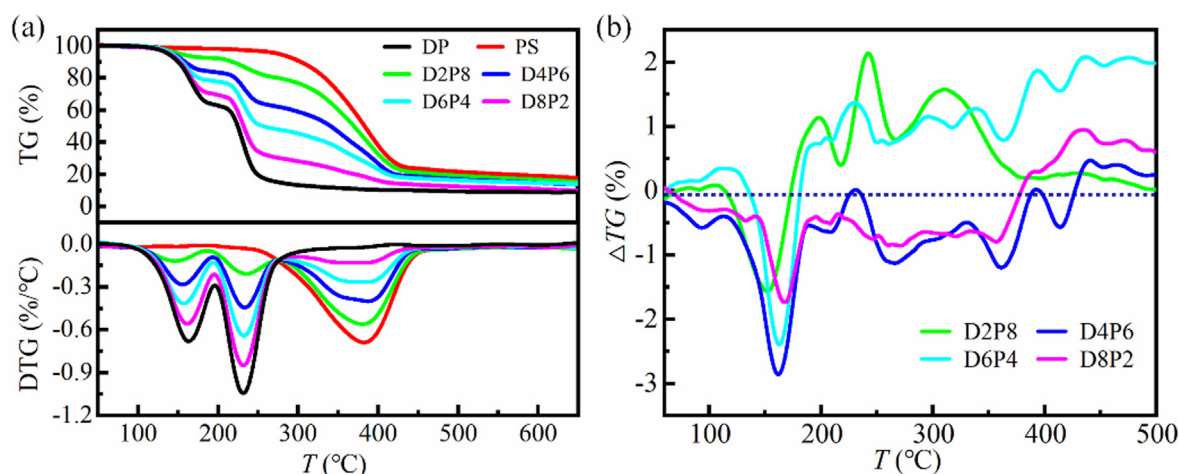


Fig. 2 Thermogravimetric analysis results at a heating rate of 20 °C·min⁻¹. (a) TG-DTG curves, (b) deviation analysis.

second stage. This indicated that the presence of PS promoted the volatilization and thermal decomposition of nitroglycerin, but had no effect on the thermal decomposition of nitrocellulose. In the third stage, the peak of DTG became gentle as the DP increased.

The deviation between the TG experimental value and the calculated value (ΔTG) for the mixtures with different DP and PS ratios was presented in Fig. 2b. For the convenience of analysis, the weight-loss process during co-pyrolysis of the mixture was combined into two stages: stage 1 (50–270 °C) and stage 2 (270–500 °C), where stage 1 corresponds to the volatilization and thermal decomposition of nitroglycerin, and the thermal decomposition of nitrocellulose in DP, and stage 2 corresponds to the release of volatile in PS. In stage 1, the ΔTG of the mixtures with different ratios was generally negative, indicating the presence of synergy. At stage 2, the ΔTG curves of the mixtures with the DP ratios of 40 wt% and 80 wt% showed a trend of first negative and then positive, indicating that the interaction was first synergistic and then inhibitory. In addition, the mixtures with the DP ratios of 20 wt% and 60 wt% ΔTG were positive, showing inhibitory effects. These interactions between DP and PS during co-pyrolysis lay the foundation for the cleaning treatment of waste EMs, indicating that this is a promising idea.

3.2. Kinetics of DP, PS and their mixtures

To evaluate the effect of different ratios on the kinetics of the mixture, the Friedman and KAS isoconversional methods were used to calculate the kinetic parameters. The activation energy (E_a) plays an important role in kinetic analysis and is referred to as the minimum energy that reactants must possess in order to carry out a specific reaction (Laougué and Merdun, 2021; Merdun and Laougué, 2021). Four heating rates of 2, 5, 10, and 20 °C·min⁻¹ were selected for TGA under an inert atmosphere (N₂), and the results were calculated by NETZSCH Kinetics Neo software. For comprehensive analysis, the weight-loss process during co-pyrolysis of the mixture was also combined into two stages: stage 1 (50–270 °C) and stage 2 (270–500 °C).

Taking the mixture with a DP ratio of 60 wt% (D6P4) as an example, the variation of mass conversion ratio (α) with temperature (T) in stage 1 and stage 2 was shown in Fig. 3a and 3b, respectively. The kinetic results of the two stages calculated by the Friedman and the KAS method were given in Fig. 3 and Fig. 4, respectively. Wherein, Fig. 3c, 3d, 4a, and 4b displayed the linear fitting results under different α , and Fig. 3e, 3f, 4c, and 4d presented the E_a - α curves obtained from the fitting lines. From Fig. 3 and Fig. 4, it can be seen that the trends of E_a with α obtained by the two methods in stage 1 and stage 2 were approximately the same. In stage 1, there were two obvious processes in the variation of E_a with α : volatilization and thermal decomposition of nitroglycerin (α less than 0.4) and thermal decomposition of nitrocellulose (α greater than 0.4). And the E_a of the latter was significantly larger than that of the former. In stage 2, E_a increased with α (0.1–0.9) and increased substantially in the later stages. This is related to the gradual decrease in volatile content and the increase in the share of carbon and ash. Carbon and ash, which are not involved in the reaction, cover the pore structure of the residue and hinder the reaction process (Liao et al., 2021), leading to a significant increase in E_a .

As well, the kinetic results for DP, PS, and their mixtures with different ratios derived from both methods were shown in Fig. 5, including E_a - α curves and average E_a -DP ratio curves. The trends obtained by Friedman and KAS methods were similar, but the former had a higher average E_a , which also reflected the difference between the differential and integral methods.

In stage 1, the average E_a of all mixtures was less than that of DP. This indicated that the addition of PS would promote the co-pyrolysis reaction. EDS experiments on ash showed the presence of the alkali metal potassium (K) in PS, which may be attributed to the catalytic effect of alkali metals in PS (Hu et al., 2017; Wang et al., 2016). In the DP ratio range of 20 %–100 %, the average E_a showed an increase, then a decrease, and then an increase with the increase of the DP ratio (the panel of Fig. 5a and 5c). The lowest average E_a was reached at 80 wt% DP (D8P2), with an average E_a of 92.6 kJ·mol⁻¹ and 83.1 kJ·mol⁻¹ obtained by Friedman and KAS methods, respectively. The complex variation of the aver-

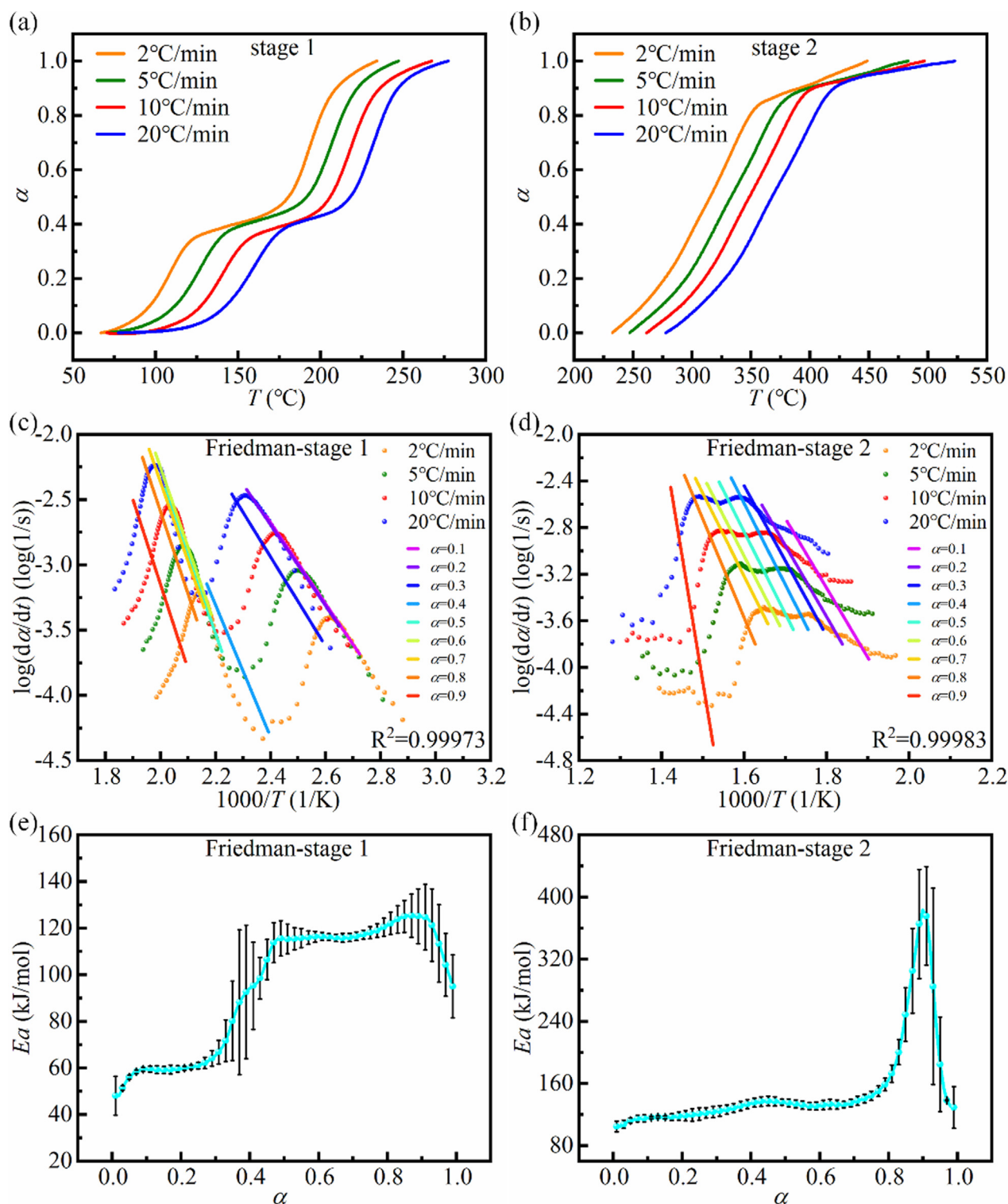


Fig. 3 Kinetic results of the mixture with a DP ratio of 60 wt% (D6P4) calculated by Friedman isoconversational method. (a), (b) α - T curves in stage 1 and stage 2. (c), (d) Fitting results at different α in stage 1 and stage 2. (e), (f) E_a - α curves in stage 1 and stage 2.

age E_a of mixtures with different mixing ratios revealed that the interaction between DP and PS was very complex. On the one hand, the alkali metal in PS promotes the pyrolysis of DP. On the other hand, the density of PS ($0.5 \text{ g}\cdot\text{m}^{-3}$) is

smaller than that of DP ($1.6 \text{ g}\cdot\text{cm}^{-3}$), and a large amount of PS wraps DP, which hinders heat transfer and diffusion (Zhou et al., 2019). The interaction of the two aspects eventually leads to complex changes in the average E_a of the mixture.

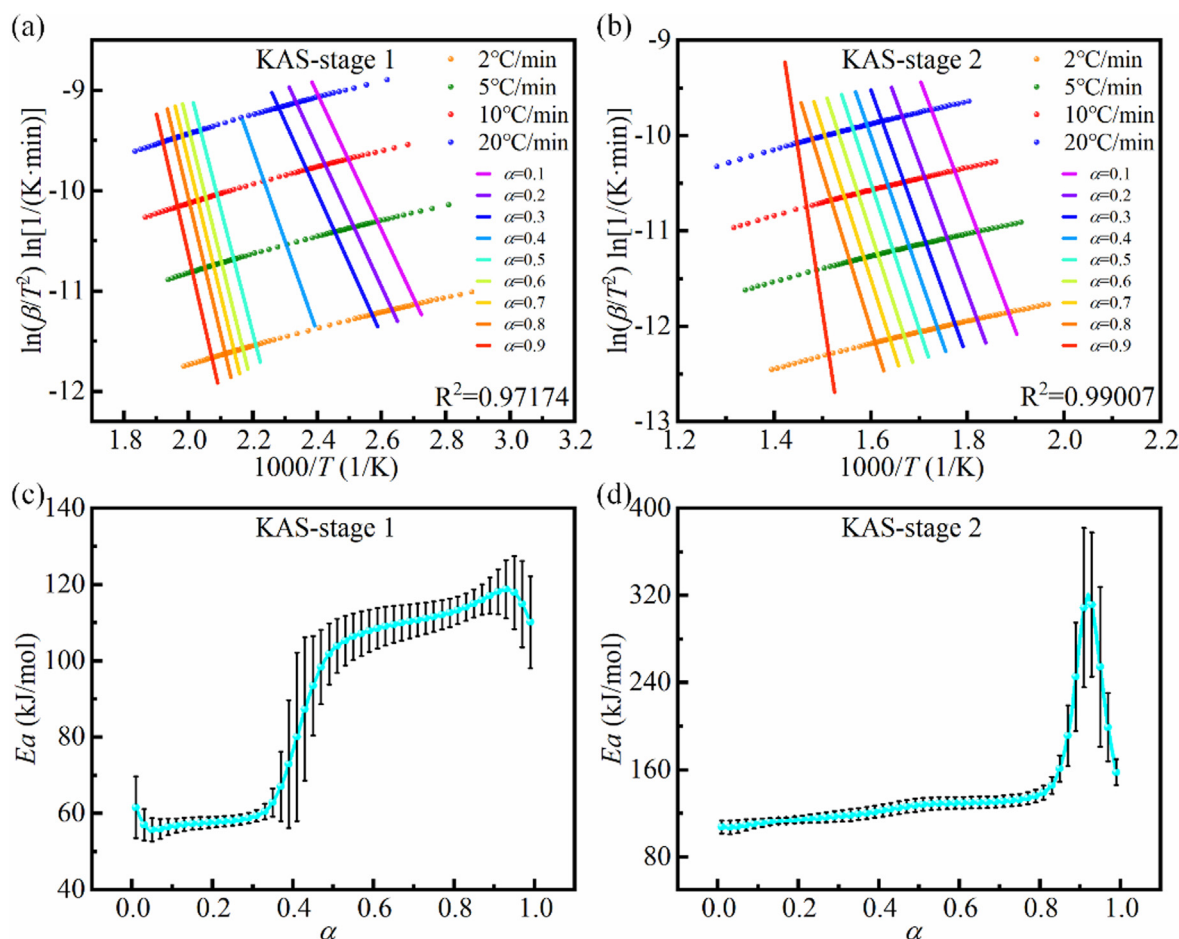


Fig. 4 Kinetic results of the mixture with a DP ratio of 60 wt% (D6P4) calculated by KAS isoconversional method. (a), (b) Fitting results at different α in stage 1 and stage 2. (c), (d) E_a - α curves in stage 1 and stage 2.

Overall, PS exerted a promotional effect on the pyrolysis process of DP.

In stage 2, it can be seen from the E_a - α curves that the trends of D8P2 (i.e., DP ratio of 80 wt%) was significantly different from the other curves. In addition, the average E_a -DP ratio curves showed that the average E_a reached the maximum when the DP ratio was 80 wt%. This may be because the residual residues (fixed carbon and ash) at the end of DP pyrolysis at stage 1 covered the pore structure of PS, hindering the reaction process at stage 2 (Liao et al., 2021). At 80 wt% DP, there were many remaining residues and the hindrance was very serious, resulting in a great change in the trend of E_a with α and a large increase in the average E_a .

Combined with Fig. 2, it can be seen that in stage 1, ΔTG , Friedman and KAS methods all indicate the synergistic effect of mixtures with different ratios. In stage 2, the average E_a of all mixtures calculated by the Friedman method was greater than that of DP, while the average E_a of mixtures calculated by the KAS method with 20 wt% and 40 wt% DP was slightly less than that of DP. Each method has certain reference values and also has some limitations. The mixtures were judged comprehensively by combining the three methods to show an overall inhibitory effect in stage 2.

In summary, the addition of PS had a synergistic effect on the pyrolysis of DP by kinetic analysis. This not only offers an

analytical approach to clarify the mechanism of the co-pyrolysis process but also provides strong theoretical support for more efficient treatment of waste EMs through co-pyrolysis with biomass.

3.3. NO_x emission characteristics during co-pyrolysis

The NO_x emission characteristics of DP, PS and their mixtures with different ratios during pyrolysis in an inert atmosphere (N₂) were investigated by fixed-bed experiments. The experimental results showed that the NO_x released from DP pyrolysis was mainly in the form of NO. This is because N in DP exists in the form of O-NO₂, and NO₂ is first released during pyrolysis. NO₂ reacts with CH₂O released during pyrolysis to form CO, NO, and H₂O (Yan et al., 2009a; Yan et al., 2009b). At the same time, NO₂ reacts rapidly with H and O radicals to transform into NO (Glarborg et al., 2018).

To determine the temperature conditions with the lowest NO_x emissions, the NO_x release curves of 50 mg DP during pyrolysis at different temperatures (400 °C, 600 °C, 800 °C, 900 °C, 1000 °C) were shown in Fig. 6a. As can be seen from the figure, the peak value of NO_x gradually decreased with the increase in temperature. Fig. 6b displayed the variation of NO_x emissions with temperature, calculated from the NO_x release curves (Fig. 6a) by Eq. (8). The results were that the

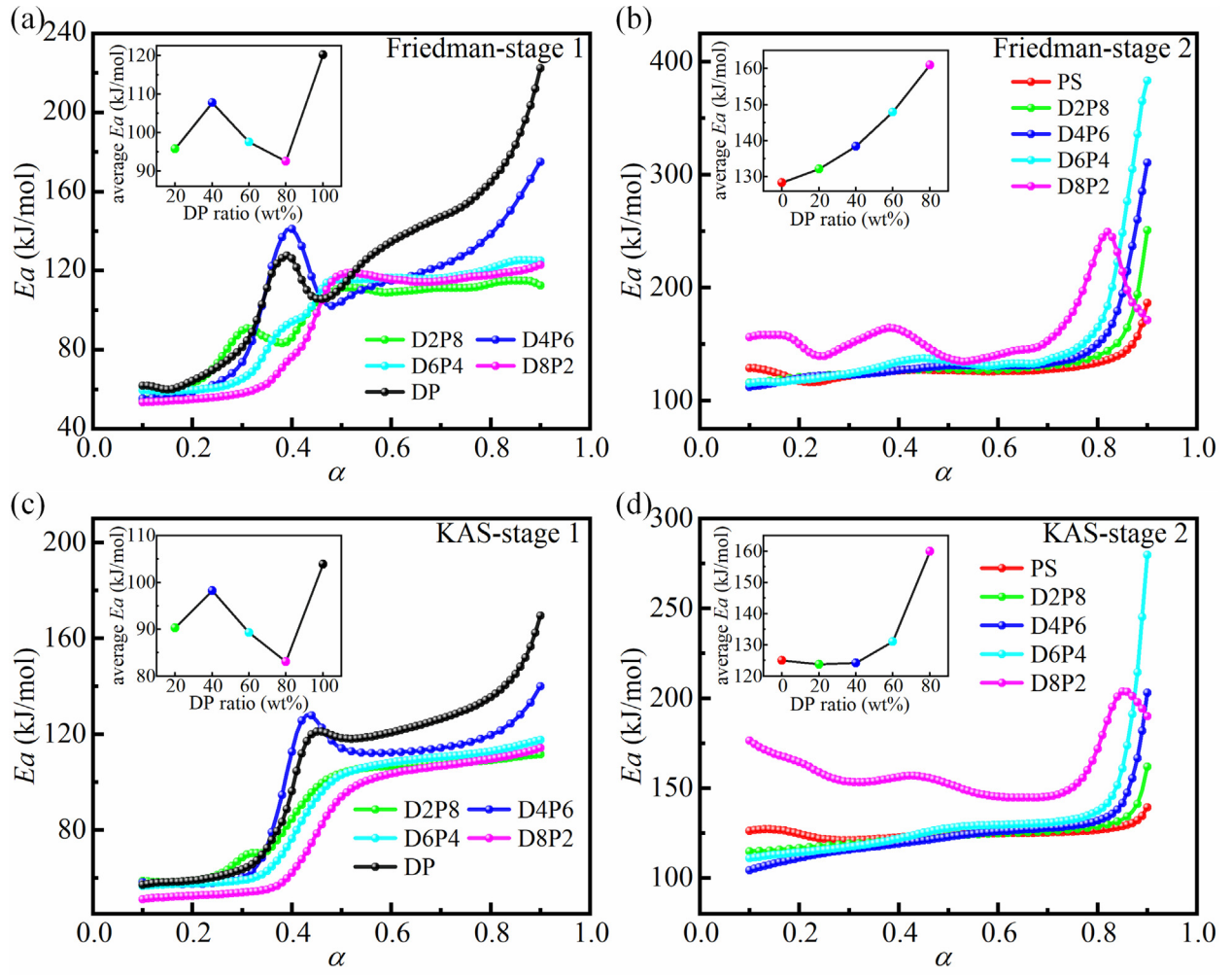


Fig. 5 Kinetic results for DP, PS, and their mixtures with different ratios calculated by Friedman and KAS isoconversional methods. (a), (c) E_a - α curves and average E_a -DP ratio curves in stage 1. (b), (d) E_a - α curves and average E_a -DP ratio curves in stage 2.

NO_x emissions decreased gradually from 19.94 mg to 11.52 mg as the temperature increased from 400 °C to 900 °C. This is mainly attributed to the increase in the reaction rate of CO, H_2 , CH_i , etc. released by pyrolysis to reduce NO to N_2 with the increase in temperature (Glarborg et al., 2018). The global reaction equation is as follows:



When the temperature increased from 900 °C to 1000 °C, the NO_x emissions increased slightly. This may be because the pyrolysis rate of DP at 1000 °C is too fast, and the residence time of pyrolysis gas in the reactor becomes shorter, resulting in a smaller reduction of NO. Therefore, 900 °C is the temperature condition with the lowest NO_x emission during DP pyrolysis alone. In the following, the interaction between DP and PS during co-pyrolysis was studied at this temperature.

The NO_x release curves of DP, PS and their mixtures with different ratios during pyrolysis at 900 °C were plotted in Fig. 6c. Compared with the NO_x emission of 50 mg DP pyrol-

ysis alone (11.52 mg), the amount of 50 mg PS was very small, only 0.58 mg. The huge difference in NO_x emissions is the reflection of the huge gap in nitrogen content between DP and PS. As can be seen from Table 1, the nitrogen content of PS was 0.12 wt%, while the nitrogen content of DP was as high as 14.91 wt%. Moreover, the lowest NO_x peak was observed for D6P4 (i.e., DP ratio of 60 wt%) among the mixtures with different ratios. With the exception of D6P4, the other ratio mixtures showed a gradual increase in the NO_x peak with the increase of the DP ratio.

To evaluate the interaction of DP and PS during co-pyrolysis, the percentage increase/decrease of actual NO_x emissions compared to the predicted values ($[\text{NO}_x]_{\text{interaction}}$) was calculated. The results were shown in Fig. 6d. It can be seen from the figure that the $[\text{NO}_x]_{\text{interaction}}$ of the mixtures were all positive, that is, the actual NO_x emissions were lower than the expected values. This meant that co-pyrolysis of DP and PS can reduce NO_x emissions, and there were synergistic effects when they were mixed in different ratios. Furthermore, with the increase of DP ratios, the synergy first increased and then decreased. When the DP ratio was 60 wt% (D6P4), the NO_x emissions reduction percentage was the highest (72.11 %), and the best synergy was achieved. This is strong

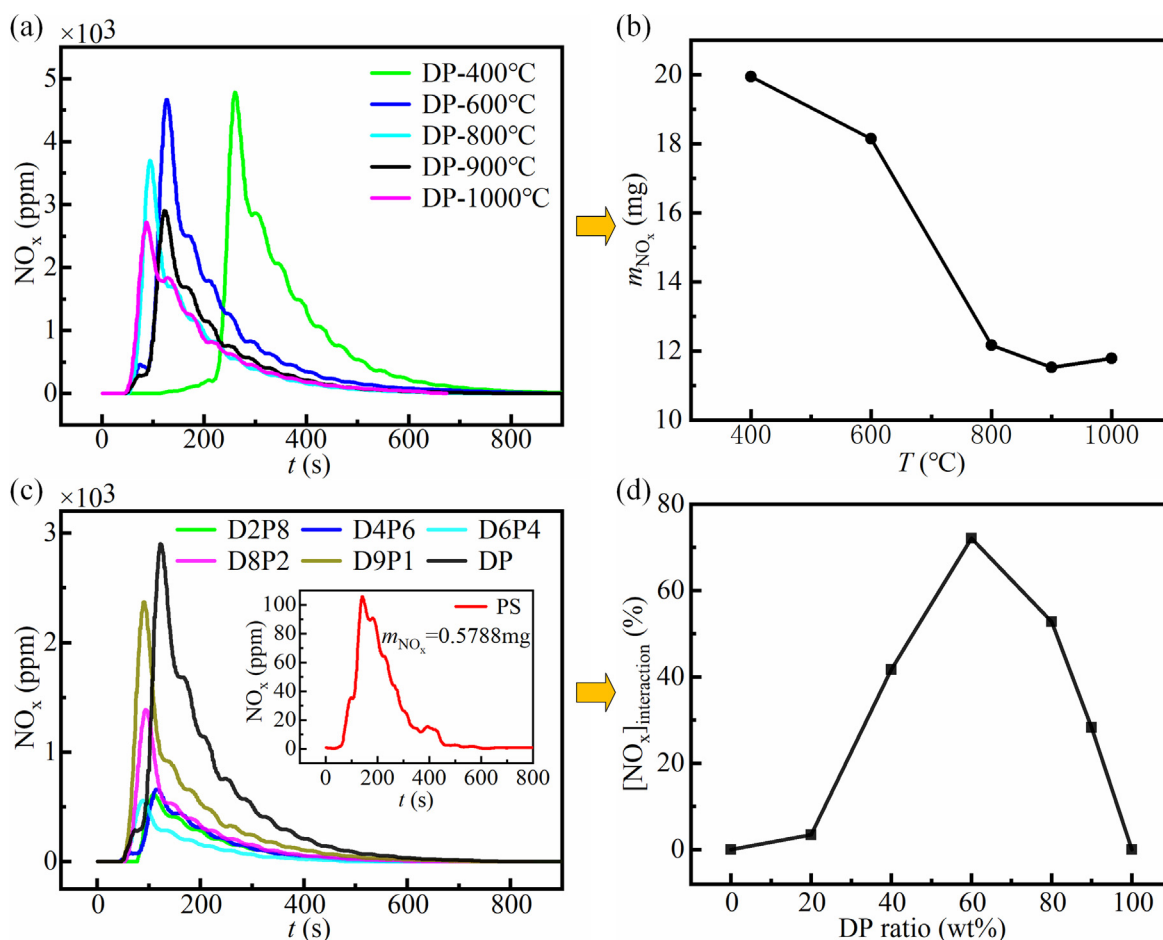


Fig. 6 (a) NO_x release curves of DP during pyrolysis at different temperatures. (b) NO_x emissions of DP during pyrolysis at different temperatures. (c) NO_x release curves of DP, PS and their mixtures with different ratios during pyrolysis at 900 °C. (d) Interaction of mixtures with different ratios in NO_x emissions.

evidence that co-pyrolysis technology with biomass has shown excellent advantages for the NO_x emissions that are a headache when treating waste EMs. This is a feasible way to treat waste EMs economically and cleanly, which is of great significance to practical engineering applications.

3.4. The proposed mechanism of interaction

The interaction mechanism of DP and PS during co-pyrolysis was investigated under the optimum conditions (900°C, DP ratio of 60 wt%). Firstly, the role of char produced by PS on NO_x emission in co-pyrolysis was determined. 20 mg PS was pyrolyzed at 900 °C in an inert environment (N₂) to produce char, which was recorded as PS-char. The obtained PS-char was mixed with 30 mg DP and co-pyrolyzed at 900°C. The NO_x release curve was given in Fig. 7a. The results showed that the NO_x emissions of the PS-char and DP mixture was reduced by 18.40 %, while that of the PS and DP mixture was reduced by 72.11 %. This suggested that PS-char played a role in reducing NO_x emissions during co-pyrolysis, which was the heterogeneous reduction mechanism of char to NO_x (Hashemi et al., 2011). However, PS-char was not the main source of synergy between DP and PS.

Then, the effect of reducing gases released during pyrolysis was studied. The release curves of CO and CH₄ during the pyrolysis of DP and PS alone were seen in Fig. 7b. It can be seen that both CO and CH₄ released by PS pyrolysis were more than those released by DP pyrolysis, especially the CH₄ increased dramatically. This indicated that PS pyrolysis would release a large amount of CO, CH_i. H₂ was also the main products of PS pyrolysis (Chen et al., 2022a). CO, CH_i and H₂ react with NO to reduce NO to N₂, resulting in lower NO_x emissions. Moreover, N in PS is mainly released in the form of NH₃ (Tchapda and Pisupati, 2014), which acts as a reducing agent and plays an important role in the denitration process (Van Caneghem et al., 2016).

In addition, it can be seen from Table 1 that the LHV of PS is higher than that of DP, and there may be a local high-temperature zone during the pyrolysis of the mixture, which accelerates the rate of the above homogeneous reaction. Char also serves as a catalyst in the above homogeneous reactions (Hashemi et al., 2011), accelerating the reaction rate. Furthermore, it has been reported that alkali metals in biomass could perform a catalytic role (Hu et al., 2017; Wang et al., 2016) to promote the reduction of NO.

Nevertheless, this does not mean that the more PS in the mixture, the better the synergy. PS has a higher O/N ratio,

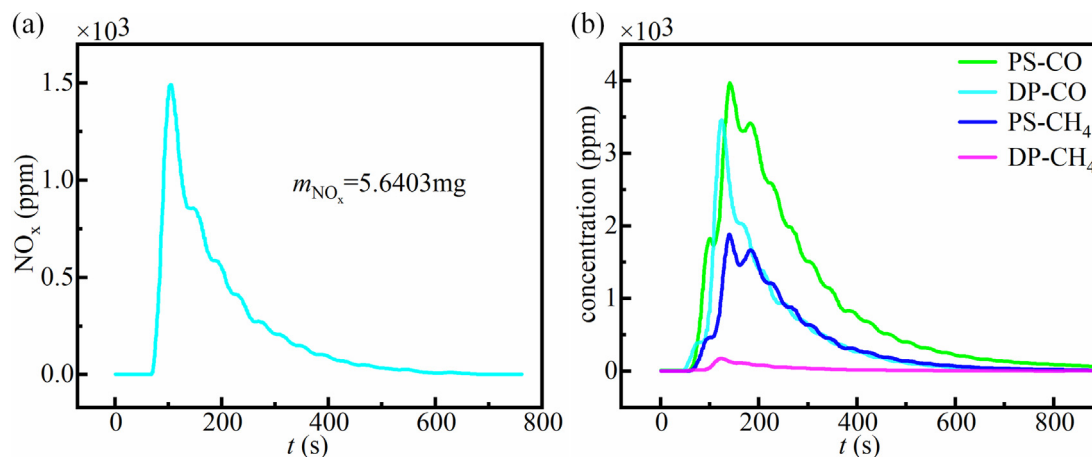


Fig. 7 (a) NO_x release curve of the mixture of char obtained by pyrolysis of 20 mg PS and 30 mg DP co-pyrolyzed at 900°C. (b) The release curves of CO and CH_4 during the pyrolysis of DP and PS alone.

which leads to the formation of more OH and O radicals during pyrolysis (Hu et al., 2017; Wang et al., 2016). These free radicals promote the conversion of N to NO (Glarborg et al., 2018), resulting in an inhibitory effect. At the pyrolysis temperature of 900 °C, the pyrolysis of DP and PS in the mixture is almost synchronous. There may be a reaction zone on the surface of the solid phase, in which the reduction of NO and the inhibition of O and OH radicals act together. Ultimately, there is an optimal mixing ratio (60 wt% DP + 40 wt% PS) that minimizes NO_x emissions. This mechanism research can help further optimize the co-pyrolysis conditions and give full play to the great advantages of co-pyrolysis technology with biomass in the treatment of waste EMs. It is worth expanding in the future.

3.5. Pyrolysis residue analysis

Morphological and surface elemental analysis of the residue after pyrolysis of the raw materials and mixtures contributes to a more comprehensive understanding of the interaction mechanisms. The morphology and surface element content obtained by SEM + EDS were shown in Figs. S1 and S2, respectively. As can be seen from Fig. S1, the microscopic morphologies of the raw material DP and PS were blocky and elongated, respectively, which reflects the differences in their structures. The microscopic morphology of the residues when DP and PS were pyrolyzed alone was similar to that of their respective raw materials. As the DP ratio increased, the morphological properties of the mixture residues tended to be that of the DP alone. Fig. S2 showed that only the raw material surface of DP contained element N, and the surface of residues after pyrolysis of PS and mixtures with different ratios (0–100 wt% DP) did not contain element N. This indicated that all the N elements of DP were released as volatile during the co-pyrolysis process, and PS was not a reduction of NO_x emissions in the form of fixed N in the residue. This also served to illustrate the interaction mechanism for the efficient NO_x emission reduction described above.

4. Conclusions and further work

The kinetics and NO_x emission characteristics of waste double-base propellant (DP) and pine sawdust (PS) during co-pyrolysis were investigated using thermogravimetric analysis and fixed-bed experiments, respectively. The following points may be concluded from the study conducted in this paper.

- (1) The kinetic analysis of Friedman and KAS isoconversional methods showed that the average activation energy of the mixtures during co-pyrolysis was smaller than that of DP pyrolysis alone. The addition of PS improved the pyrolysis reactivity of the mixture.
- (2) Fixed-bed experiments demonstrated that NO was the main form of NO_x released by DP pyrolysis alone. In the range of 400–1000 °C, the NO_x emissions for 50 mg DP alone pyrolysis gradually decreased from 19.94 mg and then slightly increased. The lowest NO_x emission was reached at 900 °C with 11.52 mg.
- (3) In the co-pyrolysis at 900 °C, the addition of PS with different ratios inhibited the NO_x emission of the mixture. At the mixture ratio of 60 wt% DP and 40 wt% PS, the best synergistic effect was achieved, and the actual NO_x emission was reduced by 72.11 % compared with the expected value.

This study shows that the co-pyrolysis of DP and PS presents significant advantages in reducing NO_x emissions, which provides an available path for clean and economical disposal of waste energetic materials. In particular, it gives a valuable reference for practical applications on an industrial scale.

Further work will study the effect of DP and PS mixtures on NO_x emission under different temperature and atmosphere conditions. Most importantly, the mechanism of NO_x emission reduction by mixing DP and PS needs to be fully studied.

Data availability

Data will be made available on request.

CRediT authorship contribution statement

Guorui Jin: Conceptualization, Methodology, Validation, Formal analysis, Writing – original draft, Writing – review & edit-

ing, Visualization. **Moru Wang:** Conceptualization, Validation, Writing – review & editing. **Jianwei Zhang:** Methodology, Writing – review & editing. **Ling Chen:** Writing – review & editing. **Xin Liao:** Writing – review & editing, Supervision. **Weidong He:** Writing – review & editing.

Declaration of Competing Interest

The authors declare that they have no known competing financial interests or personal relationships that could have appeared to influence the work reported in this paper.

Acknowledgements

Thanks to the Key Laboratory of Special Energy Materials for supporting this study.

Funding information

This research did not receive any specific grant from funding agencies in the public, commercial, or not-for-profit sectors.

Appendix A. Supplementary data

Supplementary data to this article can be found online at <https://doi.org/10.1016/j.arabjc.2023.104647>.

References

- Abelha, P., Gulyurtlu, I., Cabrita, I., 2008. Release of nitrogen precursors from coal and biomass residues in a bubbling fluidized bed. *Energ. Fuel* 22, 363–371. <https://doi.org/10.1021/ef700430t>.
- Ananiev, A.V., Istratov, A.G., Kolesnikov, V.I., Marshakov, V.N., Stesik, L.N., 1997. Solid propellant utilization by the burning propellant-coal and propellant-peat mixtures. *Int. J. Energ. Mater. Chem. Propul.* 4, 145–152. <https://doi.org/10.1615/IntJEnergeticMaterialsChemProp.v4.i1-6.170>.
- Baxter, L., Davis, K., Sinqeufield, S., Huey, S., Lipkin, J., Shah, D., Ross, J., Sclipa, G., 1996. Combustion aspects of the reapplication of energetic materials as fuels as a viable demil technology, 26. international symposium on combustion, Naples (Italy), 28 Jul-2 Aug 1996.
- Bhattacharyya, M., Shadangi, K.P., Mahanta, P., Mohanty, K., 2021. Co-pyrolysis of coal-biomass: study on reaction kinetics and thermodynamics. *Biofuel. Bioprod. Bior.* 16, 725–742. <https://doi.org/10.1002/bbb.2333>.
- Buckley, S.G., Robinson, A.L., Baxter, L.L., 1997. The reapplication of energetic materials as boiler fuels, The 5th Global Demilitarization Symposium and Exhibition.
- Budruga, P., 2018. A simple and precise differential incremental isoconversional method to kinetic analysis of heterogeneous processes under arbitrary temperature programs. *Thermochim. Acta* 661, 116–123. <https://doi.org/10.1016/j.tca.2018.01.025>.
- Chen, D., Cen, K., Zhuang, X., Gan, Z., Zhou, J., Zhang, Y., Zhang, H., 2022a. Insight into biomass pyrolysis mechanism based on cellulose, hemicellulose, and lignin: Evolution of volatiles and kinetics, elucidation of reaction pathways, and characterization of gas, biochar and bio-oil. *Combust. Flame* 242. <https://doi.org/10.1016/j.combustflame.2022.112142>.
- Chen, L., Nan, F., Li, Q., Zhang, J., Jin, G., Wang, M., Cao, X., Liu, J., He, W., 2022b. Sol-gel synthesis of insensitive nitrated bacterial cellulose/cyclotrimethylenetrinitramine nano-energetic composites and its thermal decomposition property. *Cellul.* 29, 7331–7351. <https://doi.org/10.1007/s10570-022-04730-3>.
- Chen, G., Yang, R., Cheng, Z., Yan, B., Ma, W., 2018. Nitric oxide formation during corn straw/sewage sludge co-pyrolysis/gasification. *J. Clean. Prod.* 197, 97–105. <https://doi.org/10.1016/j.jclepro.2018.06.073>.
- Cho, S., Park, C., Lee, J., Lyu, B., Moon, I., 2020. Finding the best operating condition in a novel process for explosive waste incineration using fluidized bed reactors. *Comput. Chem. Eng.* 142. <https://doi.org/10.1016/j.compchemeng.2020.107054>.
- Czajka, K.M., 2018. Proximate analysis of coal by micro-TG method. *J. Anal. Appl. Pyrol.* 133, 82–90. <https://doi.org/10.1016/j.jaap.2018.04.017>.
- Deng, L., Qiu, Y., Jiang, J., Zhu, Z., Che, D., 2022. Co-combustion characteristics of electrolytic aluminum waste and coal. *Fuel* 325. <https://doi.org/10.1016/j.fuel.2022.124890>.
- Duijm, N.J., 2002. Hazard analysis of technologies for disposing explosive waste. *J. Hazard. Mater.* 90, 123–135. [https://doi.org/10.1016/s0304-3894\(01\)00357-0](https://doi.org/10.1016/s0304-3894(01)00357-0).
- Duijm, N.J., Markert, F., 2002. Assessment of technologies for disposing explosive waste. *J. Hazard. Mater.* 90, 137–153. [https://doi.org/10.1016/s0304-3894\(01\)00358-2](https://doi.org/10.1016/s0304-3894(01)00358-2).
- Gholami, F., Tomas, M., Gholami, Z., Vakili, M., 2020. Technologies for the nitrogen oxides reduction from flue gas: A review. *Sci. Total. Environ.* 714. <https://doi.org/10.1016/j.scitotenv.2020.136712>.
- Glarborg, P., Jensen, A.D., Johnsson, J.E., 2003. Fuel nitrogen conversion in solid fuel fired systems. *Prog. Energ. Combust.* 29, 89–113. [https://doi.org/10.1016/s0360-1285\(02\)00031-x](https://doi.org/10.1016/s0360-1285(02)00031-x).
- Glarborg, P., Miller, J.A., Ruscic, B., Klippenstein, S.J., 2018. Modeling nitrogen chemistry in combustion. *Prog. Energ. Combust.* 67, 31–68. <https://doi.org/10.1016/j.peccs.2018.01.002>.
- Hashemi, H., Hansen, S., Toftegaard, M.B., Pedersen, K.H., Jensen, A.D., Dam-Johansen, K., Glarborg, P., 2011. A model for nitrogen chemistry in oxy-fuel combustion of pulverized coal. *Energ. Fuel* 25, 4280–4289. <https://doi.org/10.1021/ef200853t>.
- Hu, J., Si, Y., Yang, H., Shao, J., Wang, X., Lei, T., Agblevor, F.A., Chen, H., 2017. Influence of volatiles-char interactions between coal and biomass on the volatiles released, resulting char structure and reactivity during co-pyrolysis. *Energ. Convers. Manage* 152, 229–238. <https://doi.org/10.1016/j.enconman.2017.09.051>.
- Laouge, Z.B., Merdun, H., 2021. Investigation of thermal behavior of pine sawdust and coal during co-pyrolysis and co-combustion. *Energy* 231. <https://doi.org/10.1016/j.energy.2021.120895>.
- Li, J., Liang, X., Zhang, G., Cao, S., Liu, Z., Gu, Z., Liu, P., 2021. Shrinking particle reaction model for a waste double-base propellant during alkaline hydrolysis. *Propellants. Explos. Pyrot.* 46, 1866–1877. <https://doi.org/10.1002/prep.202100206>.
- Liao, X., Zhang, S., Wang, X., Shao, J., Zhang, X., Wang, X., Yang, H., Chen, H., 2021. Co-combustion of wheat straw and camphor wood with coal slime: Thermal behaviour, kinetics, and gaseous pollutant emission characteristics. *Energy* 234. <https://doi.org/10.1016/j.energy.2021.121292>.
- Liu, Q., Zhong, W., Yu, A., Wang, C., 2022. Co-firing of coal and biomass under pressurized oxy-fuel combustion mode in a 10 kWth fluidized bed: Nitrogen and sulfur pollutants. *Chem. Eng. J.* 450. <https://doi.org/10.1016/j.cej.2022.138401>.
- Ma, M., Liang, Y., Xu, D., Sun, S., Zhao, J., Wang, S., 2022. Gas emission characteristics of sewage sludge co-combustion with coal: Effect of oxygen atmosphere and feedstock mixing ratio. *Fuel* 322. <https://doi.org/10.1016/j.fuel.2022.124102>.
- Merdun, H., Laouge, Z.B., 2021. Kinetic and thermodynamic analyses during co-pyrolysis of greenhouse wastes and coal by TGA. *Renew. Energ.* 163, 453–464. <https://doi.org/10.1016/j.renene.2020.08.120>.
- Park, S.S., Hwang, I.S., Kang, M.S., Jeong, H.J., Hwang, J., 2016. Thermal decomposition characteristics of expired single-based propellant using a lab-scale tube furnace and a thermo-gravimetric

- analysis reactor. *J. Therm. Anal. Calorim.* 124, 657–665. <https://doi.org/10.1007/s10973-015-5231-7>.
- Peng, N., Li, Y., Liu, Z., Liu, T., Gai, C., 2016. Emission, distribution and toxicity of polycyclic aromatic hydrocarbons (PAHs) during municipal solid waste (MSW) and coal co-combustion. *Sci. Total. Environ.* 565, 1201–1207. <https://doi.org/10.1016/j.scitotenv.2016.05.188>.
- Sánchez-Jiménez, P.E., Pérez-Maqueda, L.A., Perejón, A., Criado, J. M., 2013. Generalized master plots as a straightforward approach for determining the kinetic model: The case of cellulose pyrolysis. *Thermochim. Acta* 552, 54–59. <https://doi.org/10.1016/j.tca.2012.11.003>.
- Suksankraisorn, K., Patumsawad, S., Fungtammasan, B., 2010. Co-firing of Thai lignite and municipal solid waste (MSW) in a fluidised bed: Effect of MSW moisture content. *Appl. Therm. Eng.* 30, 2693–2697. <https://doi.org/10.1016/j.applthermaleng.2010.07.020>.
- Tchapda, A., Pisupati, S., 2014. A review of thermal co-conversion of coal and biomass/waste. *Energies* 7, 1098–1148. <https://doi.org/10.3390/en7031098>.
- Ulusoy, B., Anicic, B., Lin, W., Lu, B., Wang, W., Dam-Johansen, K., Wu, H., 2021. Interactions in NO_x chemistry during fluidized bed co-combustion of residual biomass and sewage sludge. *Fuel* 294, <https://doi.org/10.1016/j.fuel.2021.120431> 120431.
- Van Caneghem, J., De Greef, J., Block, C., Vandecasteele, C., 2016. NO_x reduction in waste incinerators by selective catalytic reduction (SCR) instead of selective non catalytic reduction (SNCR) compared from a life cycle perspective: a case study. *J. Clean. Prod.* 112, 4452–4460. <https://doi.org/10.1016/j.jclepro.2015.08.068>.
- Wang, X., Deng, S., Tan, H., Adeosun, A., Vujanović, M., Yang, F., Duić, N., 2016. Synergetic effect of sewage sludge and biomass co-pyrolysis: A combined study in thermogravimetric analyzer and a fixed bed reactor. *Energ. Convers. Manage.* 118, 399–405. <https://doi.org/10.1016/j.enconman.2016.04.014>.
- Wang, M., Jin, G., He, W., Nan, F., 2022a. 3D printing of gun propellants based on laminated object manufacturing. *Mater. Manuf. Process.* 37, 1246–1256. <https://doi.org/10.1080/10426914.2022.2072884>.
- Wang, M., Jin, G., Zhou, Y., Nan, F., Lin, X., He, W., 2022b. Integration of complex geometry gun propellant form function calculation and geometry optimization. *Propellants, Explos. Pyrot.* 47. <https://doi.org/10.1002/prep.202200062>.
- Wang, Y., Liu, Y., Yang, W., Zhao, Q., Dai, Y., 2020. Evaluation of combustion properties and pollutant emission characteristics of blends of sewage sludge and biomass. *Sci. Total. Environ.* 720, <https://doi.org/10.1016/j.scitotenv.2020.137365> 137365.
- Wei, X., Liu, J.Z., Zhou, Y.N., Yuan, J.F., Zou, D.R., 2019. TG-FTIR study on waste propellants for enhanced combustion of anthracite. *Chin. J. Energ. Mater.* 27, 304–310 <https://doi.org/10.11943/CJEM2019001>.
- Yan, Q., Li, X., Wang, Y., Zhang, W., Zhao, F., 2009a. Combustion mechanism of double-base propellant containing nitrogen heterocyclic nitroamines (I): The effect of heat and mass transfer to the burning characteristics. *Combust. Flame.* 156, 633–641. <https://doi.org/10.1016/j.combustflame.2008.12.004>.
- Yan, Q., Song, Z., Shi, X., Yang, Z., Zhang, X., 2009b. Combustion mechanism of double-base propellant containing nitrogen heterocyclic nitroamines (II): The temperature distribution of the flame and its chemical structure. *Acta Astronaut.* 64, 602–614. <https://doi.org/10.1016/j.actaastro.2008.10.013>.
- Yang, X., Luo, Z., Liu, X., Yu, C., Li, Y.A., Ma, Y., 2021b. Experimental and numerical investigation of the combustion characteristics and NO emission behaviour during the co-combustion of biomass and coal. *Fuel* 287, <https://doi.org/10.1016/j.fuel.2020.119383> 119383.
- Yang, R., Ma, C., Chen, G., Cheng, Z., Yan, B., Mansour, M., 2021a. Study on NO_x emission during corn straw/sewage sludge co-combustion: Experiments and modelling. *Fuel* 285, <https://doi.org/10.1016/j.fuel.2020.119208> 119208.
- Zhou, L., Zhang, G., Reinmüller, M., Meyer, B., 2019. Effect of inherent mineral matter on the co-pyrolysis of highly reactive brown coal and wheat straw. *Fuel* 239, 1194–1203. <https://doi.org/10.1016/j.fuel.2018.11.114>.